Chicago, IL
http : //www.cigre.org

CIGRE US National Committee
2022 Grid of the Future Symposium

An Online Electromechanical Oscillation Index for a Modern Bulk Power System

[1]J.A. RICHARDS, [1]R. RATNAKUMAR,
[1,2]G.K. VENAYAGAMOORTHY
[1]Clemson University, [2]University of KwaZulu-Natal
[1]USA, [2]South Africa

SUMMARY

Continuous monitoring of electromechanical oscillations is necessary to maintain the stability of the power system. This paper describes the development of an electromechanical oscillation (EMO) index for online monitoring and analysis of electromechanical oscillations in a modern bulk power system. Time response and frequency response analysis of electromechanical oscillation data are combined using an artificial intelligence (AI) method into a single EMO index. Furthermore, the EMO indices are provided at different hierarchical levels of the power system, namely, plant level, area level, and system level. An implementation of the EMO index is illustrated on a modified two-area four-machine power system with two large solar photovoltaic plants using the real-time digital simulator. Typical results obtained from the real-time simulations shows that EMO indices can be obtained at the various levels of the power system providing near real-time situational awareness to system operators in the presence of operating condition changes and/or disturbances.

KEYWORDS

Electromechanical oscillation, index, stability, time response analysis, frequency response analysis.

johnoyr@g.clemson.edu

1. INTRODUCTION

Today's interconnected power network is dynamic and complex in nature and consists of a wide variety of nonlinear components connected to form a system, capable of generating, transmitting, and distributing electrical energy over large areas. Due to the interaction of all these components, there are many different types of dynamics in the system including electromechanical oscillations [1]. Power system electromechanical oscillations (EMO) are associated with generator rotors swinging relative to each other and are of great importance when it comes to stability [2]. Unstable low frequency electromechanical dynamics may cause large amplitude oscillations that may lead to partial system break-ups or blackout [3]. Dynamic operation of modern power system requires a continuous monitoring of low frequency electromechanical oscillations to determine the stability of the power system and its subsystems. These electromechanical oscillations must be damped in order to maintain stable operation of power systems [4].

Electromechanical oscillations in the frequency range 0.3 Hz – 2.0 Hz are inherent to power systems, and they can be classified into two categories, intra-area, and inter-area frequencies [5]. Intra-area frequencies are associated with electrically close groups of generators and are in the relatively high frequency range, mainly from 0.8 Hz – 2.0 Hz while inter-area oscillations are associated with interactions between generator groups that are electrically far apart and are in the relatively low frequency range mainly from 0.3 Hz – 0.7 Hz [2]. The low frequency electromechanical oscillations can be described by their frequencies and respective damping ratios.

Disturbances in power system mainly affects the system stability. When a significant disturbance occurs, EMO can rise and it is important that these are continuously monitored throughout different parts of the power system [6]. Because of the dynamic nature of power systems, the low frequency oscillation caused by any different types of disturbances (i.e. continuous load change, line to line or line to ground fault etc.) must be damped out quickly before it gets stronger with increasing amplitude [7]. This increasing amplitude will cause the system to go into sustained oscillation and may cause the synchronous generators to be tripped from the grid. Thus, it is crucial that some control mechanism be performed to adequately damp out these low frequency oscillations [8]. Power system stabilizers (PSSs) are installed on synchronous generators to provide adequate damping to the low frequency oscillations and as a result the angle stability gets improved efficiently. Therefore, the monitoring and studying of these dynamic properties provide substantial understanding into the signal stability properties of a power system and can be of great help for system operators [9].

Online low frequency EMO monitoring in modern power system is critical. Time response analysis (TRA) and frequency response analysis (FRA) are applied separately to monitor EMOs in power systems [10]. Online EMO monitoring using these methods separately are available today with data from synchrophasor technology. It is difficult for power system operators to determine the status of the system by only observing the TRA or FRA information of the EMOs. It is possible that TRA and FRA responses for a given EMO(s) in a power system may contain information that is not present in both analysis at the time it is presented to the system operator. A single index based on combined time response and frequency response analysis which presents accurately the online situational awareness of EMOs is needed in energy control centers, especially with the evolving power systems.

In this study, an online electromechanical oscillation (EMO) index is developed using artificial intelligence (AI) method that combines TRA and FRA which provides situational awareness to the system operator on the EMO status of the system. The primary contributions of the paper are:

- Development of electromechanical oscillation index to provide online situational awareness. The single EMO index obtained from the combination of TRA and FRA gives an indication of the damping in the power system for changes in the operating conditions and/or in the presence of disturbances.
- The availability of EMO indices at different hierarchical levels of the power system, namely system level, area levels and plant levels.

- The EMO index has been illustrated for different loading and dispatch conditions, fault durations, solar photovoltaic penetration levels, for PSSs turned on and off, and transmission line trips.

The rest of the paper is organized as follows: Section 2 describes the development of the hierarchical EMO indices. Section 3 presents the implementation of hierarchical EMO index for a modified two-area four-machine system with two solar photovoltaic plants. In Section 4, typical results and discussions are presented. Finally, the conclusion is presented in Section 5.

2. HIERARCHICAL EMO INDICIES

Power system electromechanical oscillations monitoring can be carried out at different levels including the plant, area and system levels, using TRA, FRA and the combination of TRA and FRA. The sub-sections below describe TRA, FRA, and the development of EMO indices using a combination of TRA and FRA. The integration of TRA and FRA for EMO characterization into a single index is new.

2.1 Time Response Analysis

The EMOs the system experiences after a disturbance can be analyzed using TRA. The significant parameters to determine the characteristics of the oscillation in the time domain analysis are the maximum overshoot and the settling time. The maximum overshoot is taken as the highest amplitude of the speed deviation. The bandwidth for the settling time is generally taken as 2% [11]. However, for this study on damped oscillations, the bandwidth for the settling time is limited to 0.5%.

2.2 Frequency Response Analysis

Another method to analyze EMOs after a disturbance is the FRA. The Prony method is a commonly used method to carry out frequency response analysis. Prony analysis provides the amplitude, damping, phase, and frequency contained in a signal and is perhaps the method for which more extensive results and applications have been reported in the power system literature [12] & [13]. This method of fitting a linear combination of exponential terms to a signal can be observed in (1).

$$f(t) = \sum_{i=1}^{N} Ae^{\sigma_i t} \cos(\omega_i t + \varphi_i) \qquad i = 1,2,3 \ldots, N \tag{1}$$

Where, A is the amplitude, σ is the damping coefficient, ω is the frequency in radians and ϕ is the phase angle. From (1), the damping ratio for the frequencies embedded within the signal can be calculated using the following equation.

$$\varepsilon = -\frac{\sigma}{\sqrt{\sigma^2 + \omega^2}} \tag{2}$$

The basic steps to carry out the Prony analysis is as follows:

i. Construct a linear prediction model from the measurement signals of the synchronous generators.
ii. Find the roots of the polynomial associated with the linear prediction model.
iii. Determine the damping coefficients and frequencies from the roots.
iv. Determine the damping ratio using the frequencies and their associated damping coefficients.

The advantage of the Prony method is that it converts a non-linear approximation of exponential sums by solving a set of linear equations and a root-finding problem [10].

2.3 Integration of TRA and FRA

The Takagi Sugeno fuzzy logic is used to determine the EMO index by combining the TRA and FRA. Fuzzy logic consists of three steps: fuzzification, inference, and defuzzification. Fuzzification is the process of converting crisp input values into fuzzy concepts with associated membership functions. The inference technique involves reasoning using predefined fuzzy logic rules. Defuzzification is the process of converting the reasoning procedure's output into crisp values. Defuzzification is unnecessary when the output of the fuzzy is crisp [14]. The normalized values of the parameters obtained from the TRA, and FRA are used as the inputs of the fuzzy logic system. The normalization was implemented such that zero and one represent poor and ideal system status, respectively. The supplemental values of the normalized maximum overshoot and settling time are used as the fuzzy inputs because EMOs with less than maximum overshoot and settling time have better system stability status. The inputs are associated to three triangular membership functions. The inputs are associated to three triangular membership functions. First function is a decreasing function that ranges from 0 to 0.5, the second function is a combination of increasing and decreasing functions respectively from 0 to 0.5 and from 0.5 to 1. Third function is an increasing function from 0.5 to 1.

The input levels are used to define the rules. Since there are four inputs and each input have three levels, 81 rules as can be defined as shown in Table I. As each input is given same level of significance, the logics to define the rules will become 15. As shown in Tables I and II, the four input levels were added up and normalized based on the assigned values (H=2, M=1, L=0) for each input level.

Table I. Fuzzy Logic to Define Rules

Rule No.	Max Overshoot	Settling time	Inter-area Damping	Intra-area Damping	Output	Output Level
1	L	L	L	L	0	Zero
2	L	L	L	M	0.125	VVL
3	L	L	L	H	0.25	VL
4	L	L	M	L	0.125	VVL
5	L	L	M	M	0.25	VL
6	L	L	M	H	0.375	L
:	:	:	:	:	:	:
:	:	:	:	:	:	:
:	:	:	:	:	:	:
78	H	H	M	H	0.875	VVH
79	H	H	H	L	0.75	VH
80	H	H	H	M	0.875	VVH
81	H	H	H	H	1	Perfect

Table II. Fuzzy Rules

No.	H	M	L	Total	Output	Output Level
1	0	0	4	0	0	Zero
2	0	1	3	1	0.125	VVL
3	0	2	2	2	0.25	VL
4	0	3	1	3	0.375	L
5	0	4	0	4	0.5	M
6	1	0	3	2	0.25	VL
7	1	1	2	3	0.375	L
8	1	2	1	4	0.5	M
9	1	3	0	5	0.625	L
10	2	0	2	4	0.5	M
11	2	1	1	5	0.625	H
12	2	2	0	6	0.75	VH
13	3	0	1	6	0.75	VH
14	3	1	0	7	0.875	VVH
15	4	0	0	8	1	Perfect

2.4 EMO Indices at Different Power System Levels

To develop the hierarchical EMO indices, aggregated signals for the plant, area and system needs to be calculated from the individual generator measurements. For this study, the individual generator measurements are speed deviation signals. Equation (3) shows us the aggregation of the speed deviation at the plant level using the speed deviation and inertia data of the generators in the respective plants.

$$\Delta\omega_P = \frac{\sum_{g=1}^{n} H_g \Delta\omega_g}{\sum_{g=1}^{n} H_g} \quad (3)$$

Where, H_g and $\Delta\omega_g$ are the inertia and speed deviation of each individual generator, g, in a power plant, P, respectively.

Likewise, using equations (4a) and (4b) the aggregated speed deviation signal of the generators in an area are computed using the speed deviation, $\Delta\omega_P$ (obtained using (3)) and inertia data, H_P, of the respective plants which are in the particular area.

$$\Delta\omega_A = \frac{\sum_{p=1}^{n} H_P \Delta\omega_P}{\sum_{P=1}^{n} H_P} \tag{4a}$$

$$H_P = \sum_{1}^{n} H_g \tag{4b}$$

Finally, equation (5a) and (5b) shows us the calculation of the speed deviation of the system using the speed deviation, $\Delta\omega_A$ (obtained using (4a)) and inertia data, H_A of the area which are in the system.

$$\Delta\omega_S = \frac{\sum_{A=1}^{n} H_A \Delta\omega_A}{\sum_{A=1}^{n} H_A} \tag{5a}$$

$$H_A = \sum_{P=1}^{n} H_P \tag{5b}$$

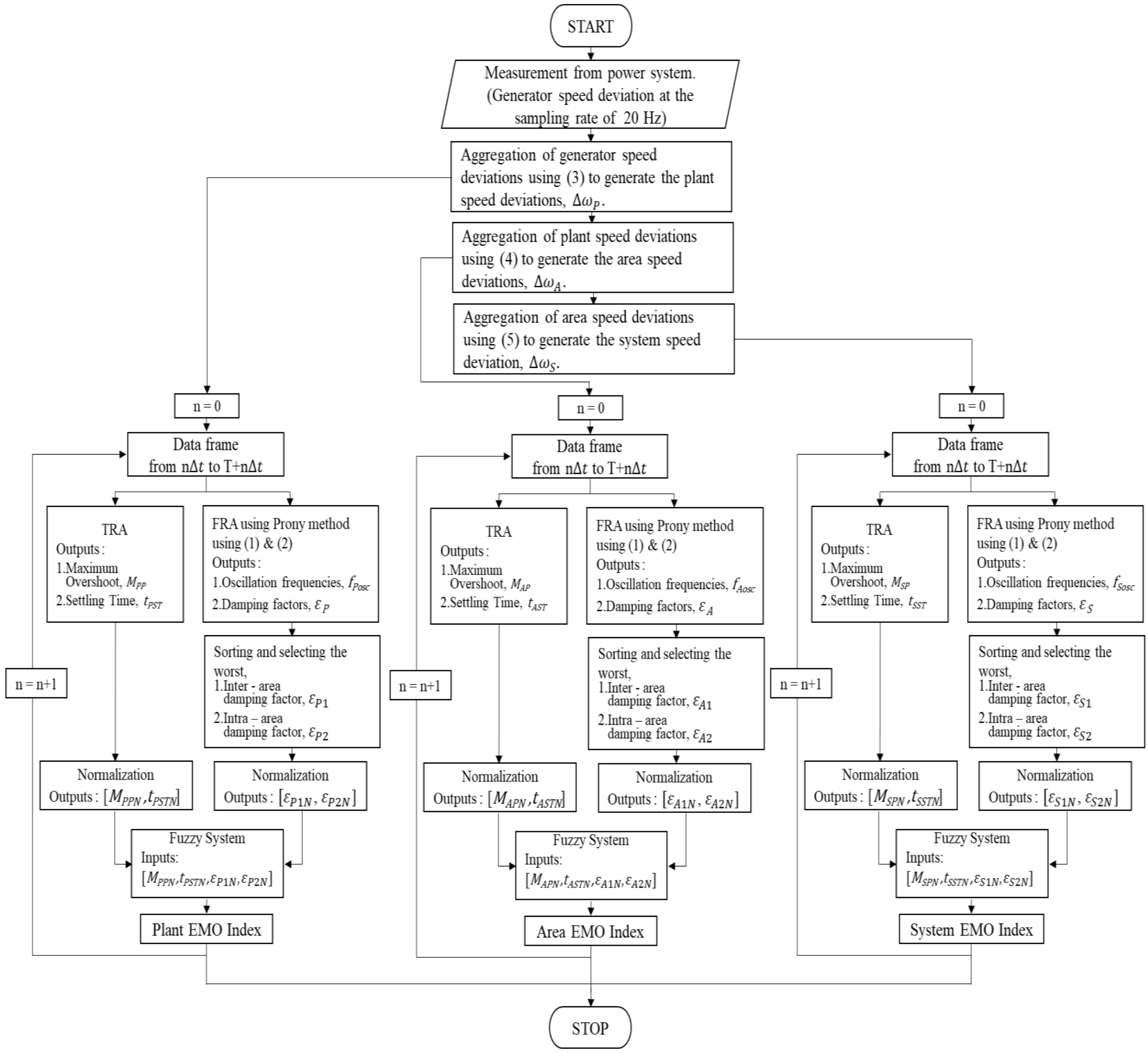

Figure 1. Schematic flowchart for online EMO indices of different levels of the power system

The overall procedure for computing the EMO indices at the different levels is shown in Fig. 1. Where, T represents the window size of the speed deviation data and Δt is the time window updating step size.

3. IMPLEMENTATION OF HIERARCHICAL EMO INDEX

3.1 Modified two-area four-machine power system

The modified two-area four-machine system shown in Fig. 2. was implement on a real time used to illustrate the EMO index. The system has four power plants and two solar photovoltaic power plants in two areas. This power system was simulated in real time on the real-time digital simulator (RTDS). The system was tested for different disturbances at different loading and dispatch condition for PSSs turned on and off. The ratings of the power plants and different operation conditions are shown in Table III.

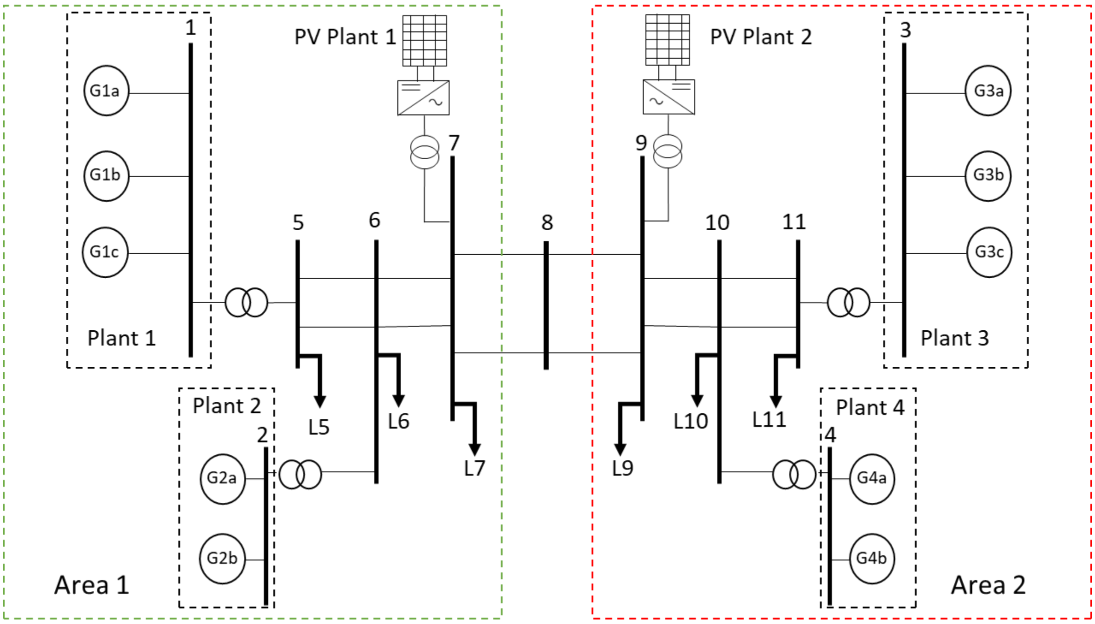

Figure 2. Modified two-area four-machine power system

Table II. Generation and Load Data

Plant Parameters		**Generation**							**Load**							**Power Transfer Area 1 to Area 2**
		Area 1			**Area 2**			**Total**	**Area 1**			**Area 2**			**Total**	
		P1	**P2**	**PV 1**	**P3**	**P4**	**PV 2**		**Bus 5**	**Bus 6**	**Bus 7**	**Bus 9**	**Bus 10**	**Bus 11**		
Inertia (s)		9	6.4	-	10.4	5.3	-									
Rating (MW)		900	900	600	900	900	600									
Loading Condition	High (MW)	627	627	136	632	613	136	**2771**	557	251	170	553	712	506	**2749**	410
	Medium (MW)	445	445	136	461	440	136	**2063**	415	186	125	520	525	375	**2146**	307
	Light (MW)	270	270	140	160	142	136	**1118**	300	110	70	210	225	200	**1115**	201

3.2 Implementation of the Hierarchical EMO Indices

The TRA (maximum overshoot and settling time) and FRA (inter-area and intra-area damping factor) for the different loading conditions with PSSs turned on and off was experimentally gathered for different fault positions and fault durations. According to the gathered data the normalization factor for each plant, area and system was obtained. The normalized values for the TRA and FRA were calculated using these normalizing factors. The EMO index was obtained for several cases by changing the operating condition changes and/or disturbances. Here, the window size T was taken as 15 s and the updating time step Δt was taken as 1 s.

4. RESULTS AND DISCUSSION

The EMO index has been illustrated for different loading and dispatch conditions, fault durations, solar photovoltaic penetration levels, for PSSs turned on and off, and transmission line trips. Six case studies were carried out to analyse the performance of the EMO indices.

Case (i): EMO indices for different loading conditions

Fig. 3 displays the speed deviation of Plant 2 under heavy, medium, and light loading conditions when a 10 cycles fault is applied at the Plant 4 bus. The graph demonstrate that the EMO index is better under light loading condition. Table III in Appendix 1 shows a 10 cycles fault at different locations. The hierarchical EMO indices are in the green zone under light loading condition and tends to move to the yellow and red zones under heavy load.

Case (ii): EMO indices for different fault durations

The Fig. 4 shows the speed deviation of Plant 2 for 10 cycles and 6 cycles faults applied at Plant 4 bus with the PSSs turned on. A better EMO index was observed for the 6 cycles fault. Table IV in Appendix 1 shows the EMO indices recorded for a 6 cycles fault for heavy loading condition with all PSSs turned on and off. We can see that the EMO indices have higher index values than the 10 cycles fault in case (i).

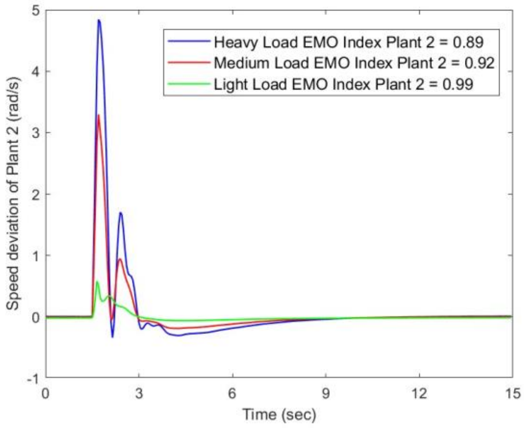

Figure 3. Speed deviation of Plant 2 with 10 cycles fault at Plant 4 for heavy/medium/light loading conditions with PSSs turned on

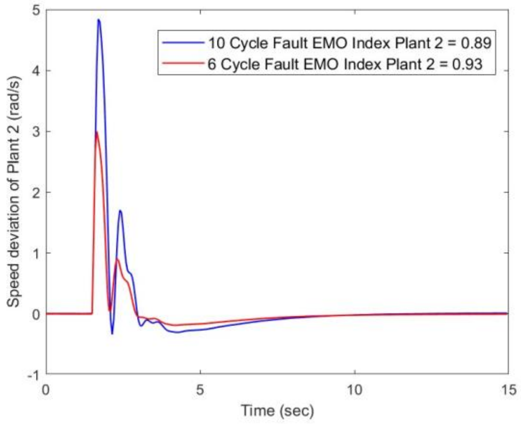

Figure 4. Speed deviation of Plant 2 with 10/6 cycles faults at Plant 4 with PSSs turned on - heavy loading condition

Case (iii): EMO indices for a 10 cycles fault for different solar photovoltaic penetration levels

Fig. 5 shows the speed deviation of Plant 2 when there is a 10 cycles fault applied at Plant 2 bus with high and low solar photovoltaic penetration. With low solar photovoltaic penetration, the EMO index for Plant 2 moves towards the critical zone. Table V in Appendix 1 displays the hierarchical EMO indices recorded for different level of solar photovoltaic penetration. When solar generation is high, the EMO indices are in the green zone while with low solar generation the EMO indices tend towards the yellow and red zones. It indicates that the generators are getting more loaded in the absence of solar power so there will be a high accelerating power when a fault occurs that is reflected in the EMO indices.

Case (iv): EMO indices for 10 cycles fault with PSSs turned on and off

Fig. 6 displays the speed deviation of Plant 2 in the scenarios with the PSSs turned on and off when a 10 cycles fault is applied at the Plant 4 bus. The EMO index that was obtained with the PSSs turned on is noticeably better than the EMO index that was obtained with the PSSs turned off, demonstrating that the PSSs has enhanced system stability in this instance, and it is reflected through the EMO indices. The tables in the Appendix 1 shows the EMO indices for PSSs turned on and off for all different cases.

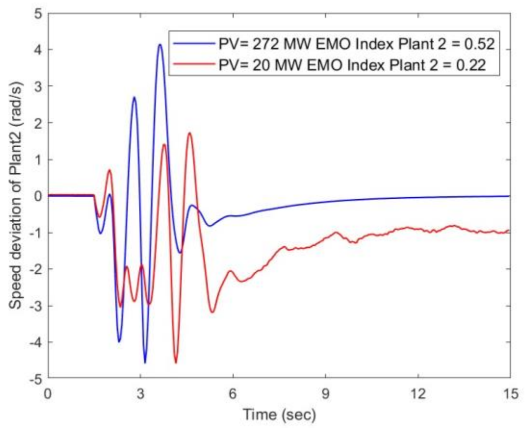

Figure 5. Speed deviation of Plant 2 with 10 cycles fault at Plant 4 with PSSs turned on with solar PV 272 MW/20 MW - heavy loading condition

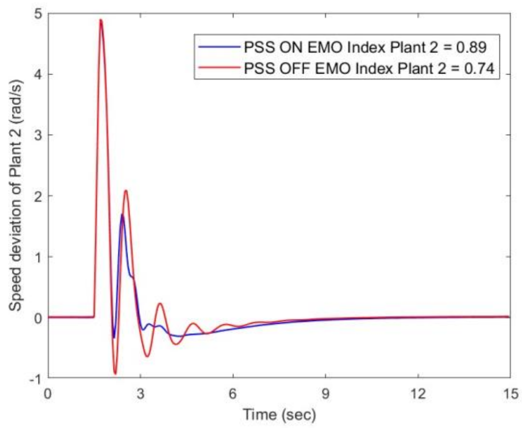

Figure 6. Speed deviation of Plant 2 with 10 cycles fault at Plant 4 with PSSs turned on and off - heavy loading condition

Case (v): EMO indices for a line loss with PSSs turned on and off

Fig. 7 is showing the speed deviation of Plant 2 when there is a line loss between bus 8 & 9 with PSSs turned on and off. Here also, the EMO index is better with the PSSs turned on. Table VI in Appendix 1 shows mostly green which indicates that a line loss does not greatly impact the EMO index.

Case (vi): EMO situational awareness-based generation dispatch

Fig. 8 shows the speed deviation of Plant 2 when a 10 cycles fault is applied at Plant 2 bus when the dispatch between Plant 1 and Plant 2 is equal and when it is 60% - 40%. The solar photovoltaic generation was kept low at 20MW. Here, we can see that the change in the dispatch has improved the EMO index of the Plant 2. Even though the ratings of the power Plant 1 and power Plant 2 are equal, power Plant 2 has significantly less inertia which causes it to oscillate more under disturbance as shown in Table VII of Appendix 1. Therefore, the EMO index improves when the 60% - 40% dispatched is applied.

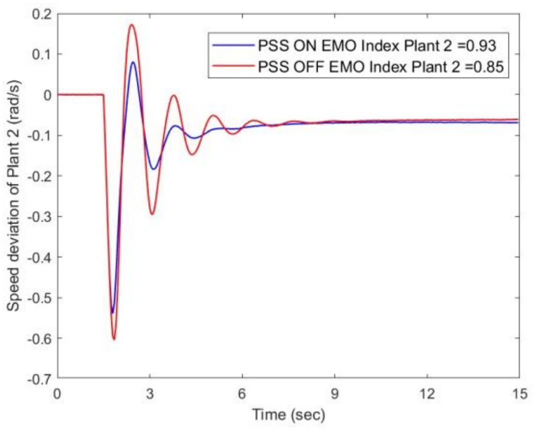

Figure 7. Speed deviation of Plant 2 for a line loss between Bus 8 and Bus 9 at heavy loading condition with PSSs turned on and off

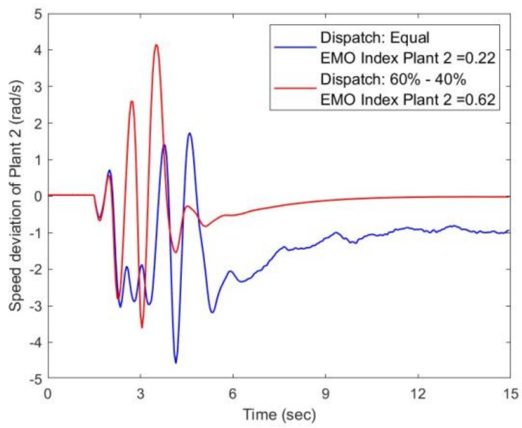

Figure 8. Speed deviation of Plant 2 with a 10 cycles fault at Plant 2 for Equal/60% - 40% Dispatch between Plant 1 and Plant 2 with PSSs turned on - heavy loading condition

5. **CONCLUSION**

Modern power systems are evolving because of high penetration of renewable energy sources and the integration of smart technologies. As a result, it is important to monitor the EMO in the system. This paper has described about an approach that combined both TRA and FRA using fuzzy logic to develop a single EMO index that provides online situational awareness to system operators of utility control centres. EMO indices were introduced at different power system levels in the hierarchy, namely system, area, and plant levels. The hierarchical EMO indices were illustrated and proven to reflect the damping of the EMOs in the power system. This hierarchical EMO index values for different operating conditions can be used by the system operator to monitor the EMOs in different levels of a power system.

Future works include taking direct measurements from the phasor measurement units, optimizing the time window utilized to TRA and FRA, and parallelizing the computation engine of the TRA, FRA, and EMO indices at various levels of the power system. Furthermore, prediction methods can be applied to provide EMO index in real-time. The EMO indices can be utilized to tune PSSs as well as implement stability constraint dispatch for power system. Moreover, there are potential applications in demand response management of this EMO indices.

ACKNOWLEDGEMENT

Funding: This research was funded by US NSF grants CNS 2131070 and the Duke Energy Distinguished Professor Endowment Fund.

BIBLIOGRAPHY

[1] J.H. Chow (Ed.), “Time-Scale Modeling of Dynamic Networks with Applications to Power Systems,” NewYork: Springer-Verlag, 1982.

[2] M. Klein, G. J. Rogers, and P. Kundur, “A Fundamental Study of Inter-Area Oscillations in Power Systems,” IEEE Transactions on Power Systems, vol. 6, no. 3, pp. 914-921, Aug. 1991.

[3] Hauer, A.J.F., Trudnowski, D.J., and DeSteese, J.G. (2007) “A Perspective on WAMS Analysis Tools for Tracking of Oscillatory Dynamics,” In Proceedings of the IEEE Power Engineering Society General Meeting, June 2007.

[4] Sauer PW, Pai MA. Power system dynamics and stability, (Prentice Hall, Upper Saddle River), 1998.

[5] Rogers G. Power system oscillations. (Kluwer Academic, Boston), 2000.

[6] T. Hashiguchi, M. Yoshimoto, Y. Mitani, O. Saeki and K. Tsuji, "Oscillation mode analysis in power systems based on data acquired by distributed phasor measurement units", Proc. Int. Symp. Circuits Systems, vol. 3, pp. 367-370, 2003-May-25.

[7] Z. Bao-Hui, L. Cheng, Z. Hao, A. Klimek, B. Zhiqian, Y. Deng, G. Yao, and J. Shu, "Study on security protection of transmission section to prevent cascading tripping and its key technologies," in IEEE/PES Transmission and Distribution Conference and Exposition: Latin America, Bogota, pp. 1-13, 13-15 Aug. 2008.

[8] S. Sheetekela, and K. A. Folly, "Multimachine power system stabilizer design based on evolutionary algorithm," in 44th International Universities’ Power Engineering Conference, Glasgow, Scotland, 1-4 Sept. 2009.

[9] Hauer J.F.: ‘Application of Prony analysis to the determination of modal content and equivalent models for measured power system response’, IEEE Trans. Power Syst., 1991, 6, (3) , pp. 1062–1068.

[10] John W. Pierre, Ning Zhou, Manu Parashar, Daniel Trudnowski and John Hauer, Performance of Three Mode-Meter Block Processing Algorithms for Automated Dynamic Stability Assesment", IEEE Trans. Power Syst, VOL. 23, NO.2, 2008.

[11] Kuo, C.K., Golnaraghi, F. Automatic control systems, 8th ed. (Willey). 2003.

[12] Venayagamoorthy G.K., Aliyu U.O., Chow J.H., Sanchez-Gasca J.J., Modal extraction with three different methods for the Nigerian power system, may 2005.

[13] Rodríguez A.F., de Santiago Rodrigo L., Guillén L.E., Ascariz J.M.: Coding prony’s method in matlab and applying it to biomedical signal filtering, IET Gener, Transm. Distrib., 2018,1, (2), pp. 2-12.

[14] J. Lu, M.H. Nehrir*, D.A. Pierre.: A fuzzy logic-based self tuning power system stabilizer optimized with a genetic algorithm. Electric Power Systems Research 60 (2001) 77–83.

APPENDIX 1

Table III. EMO indices for 10 cycles fault

Electromechanical Oscillation Index (EMO Index)												PV Integration = 272 MW			
Loading Condition	Fault Location	Plant 1 EMO Index		Plant 2 EMO Index		Plant 3 EMO Index		Plant 4 EMO Index		Area 1 EMO Index		Area 2 EMO Index		System EMO Index	
		PSS ON	PSS OFF	PSS ON	PSS OFF	PSS ON	PSS OFF	PSS ON	PSS OFF	PSS ON	PSS OFF	PSS ON	PSS OFF	PSS ON	PSS OFF
Heavy	No Fault	1.00	1.00	1.00	1.00	1.00	1.00	1.00	1.00	1.00	1.00	1.00	1.00	1.00	1.00
	Plant 1	0.54	0.14	0.53	0.12	0.65	0.21	0.67	0.09	0.53	0.17	0.60	0.21	0.48	0.09
	Plant 2	0.51	0.11	0.52	0.12	0.67	0.18	0.64	0.09	0.53	0.14	0.60	0.19	0.25	0.08
	Plant 3	0.83	0.74	0.89	0.74	0.78	0.64	0.79	0.71	0.89	0.70	0.67	0.66	0.56	0.57
	Plant 4	0.89	0.72	0.89	0.74	0.80	0.72	0.76	0.68	0.89	0.74	0.73	0.65	0.67	0.55
	Bus 8	0.93	0.79	0.85	0.79	0.94	0.79	0.94	0.81	0.89	0.80	0.91	0.84	0.86	0.77
Light	No Fault	1.00	1.00	1.00	1.00	1.00	1.00	1.00	1.00	1.00	1.00	1.00	1.00	1.00	1.00
	Plant 1	0.88	0.95	0.94	0.96	0.96	0.95	0.85	0.83	0.96	0.92	0.94	0.94	0.97	0.97
	Plant 2	0.96	0.88	0.91	0.95	0.81	0.92	0.90	0.77	0.96	0.96	0.93	0.87	0.97	0.92
	Plant 3	0.98	0.95	0.92	0.91	0.87	0.87	0.97	0.97	0.93	0.91	0.96	0.89	0.94	0.93
	Plant 4	0.98	0.99	0.99	0.99	0.98	0.97	0.97	0.95	0.97	0.87	0.97	0.97	0.92	0.95
	Bus 8	0.90	0.90	0.94	0.98	0.96	0.96	0.95	0.95	0.98	0.98	0.94	0.94	0.87	0.97

Table IV. EMO indices for 6 cycles fault

Electromechanical Oscillation Index (EMO Index)												PV Integration = 272 MW			
Loading Condition	Fault Location	Plant 1 EMO Index		Plant 2 EMO Index		Plant 3 EMO Index		Plant 4 EMO Index		Area 1 EMO Index		Area 2 EMO Index		System EMO Index	
		PSS ON	PSS OFF	PSS ON	PSS OFF	PSS ON	PSS OFF	PSS ON	PSS OFF	PSS ON	PSS OFF	PSS ON	PSS OFF	PSS ON	PSS OFF
Heavy	No Fault	1.00	1.00	1.00	1.00	1.00	1.00	1.00	1.00	1.00	1.00	1.00	1.00	1.00	1.00
	Plant 1	0.78	0.73	0.89	0.82	0.88	0.67	0.89	0.77	0.87	0.81	0.79	0.75	0.82	0.67
	Plant 2	0.58	0.17	0.63	0.19	0.53	0.09	0.58	0.12	0.58	0.17	0.51	0.11	0.40	0.15
	Plant 3	0.83	0.77	0.86	0.71	0.80	0.80	0.86	0.72	0.83	0.79	0.74	0.74	0.78	0.64
	Plant 4	0.93	0.85	0.93	0.76	0.87	0.63	0.80	0.61	0.93	0.69	0.82	0.57	0.77	0.66
	Bus 8	0.86	0.76	0.96	0.77	0.96	0.84	0.88	0.82	0.96	0.78	0.83	0.87	0.92	0.78

Table V. EMO indices with different solar photovoltaic integrations

Electromechanical Oscillation Index (EMO Index)															
Solar PV Integration	Fault Location	Plant 1 EMO Index		Plant 2 EMO Index		Plant 3 EMO Index		Plant 4 EMO Index		Area 1 EMO Index		Area 2 EMO Index		System EMO Index	
		PSS ON	PSS OFF	PSS ON	PSS OFF	PSS ON	PSS OFF	PSS ON	PSS OFF	PSS ON	PSS OFF	PSS ON	PSS OFF	PSS ON	PSS OFF
272 MW	No Fault	1.00	1.00	1.00	1.00	1.00	1.00	1.00	1.00	1.00	1.00	1.00	1.00	1.00	1.00
20 MW		1.00	1.00	1.00	1.00	1.00	1.00	1.00	1.00	1.00	1.00	1.00	1.00	1.00	1.00
272 MW	Plant 1	0.54	0.14	0.53	0.12	0.65	0.21	0.67	0.09	0.53	0.17	0.60	0.21	0.48	0.09
20 MW		0.59	0.16	0.62	0.15	0.64	0.10	0.67	0.11	0.66	0.16	0.61	0.07	0.42	0.07
272 MW	Plant 2	0.51	0.11	0.52	0.12	0.67	0.18	0.64	0.09	0.53	0.14	0.60	0.19	0.25	0.08
20 MW		0.27	0.00	0.22	0.00	0.33	0.04	0.36	0.05	0.27	0.00	0.26	0.04	0.12	0.07
272 MW	Plant 3	0.83	0.74	0.89	0.74	0.78	0.64	0.79	0.71	0.89	0.70	0.67	0.66	0.56	0.57
20 MW		0.72	0.79	0.88	0.63	0.78	0.53	0.76	0.52	0.88	0.79	0.56	0.45	0.50	0.42
272 MW	Plant 4	0.89	0.72	0.89	0.74	0.80	0.72	0.76	0.68	0.89	0.74	0.73	0.65	0.67	0.55
20 MW		0.74	0.72	0.85	0.55	0.74	0.58	0.64	0.37	0.85	0.69	0.72	0.42	0.50	0.52
272 MW	Bus 8	0.93	0.79	0.85	0.79	0.94	0.79	0.94	0.81	0.89	0.80	0.91	0.84	0.86	0.77
20 MW		0.88	0.76	0.92	0.69	0.86	0.82	0.81	0.65	0.92	0.78	0.87	0.67	0.73	0.54

Table VI. EMO indices for a line loss between Bus 8 & 9

Electromechanical Oscillation Index (EMO Index)											PV Integration = 272 MW			
Loading Condition	Plant 1 EMO Index		Plant2 EMO Index		Plant 3 EMO Index		Plant 4 EMO Index		Area 1 EMO Index		Area 2 EMO Index		System EMO Index	
	PSS ON	PSS OFF	PSS ON	PSS OFF	PSS ON	PSS OFF	PSS ON	PSS OFF	PSS ON	PSS OFF	PSS ON	PSS OFF	PSS ON	PSS OFF
Heavy	0.99	0.93	0.95	0.93	0.91	0.83	0.98	0.86	0.99	0.92	0.98	0.91	0.99	0.89
Light	1.00	0.99	1.00	0.99	0.99	0.93	0.99	0.92	0.95	1.00	0.99	0.90	1.00	1.00

Table VII. EMO indices with different dispatches of Plant 1 and Plant 2

Electromechanical Oscillation Index (EMO Index)												PV Integration = 20 MW			
Dispatch Plant1 - Plant2	Fault Location	Plant 1 EMO Index		Plant 2 EMO Index		Plant 3 EMO Index		Plant 4 EMO Index		Area 1 EMO Index		Area 2 EMO Index		System EMO Index	
		PSS ON	PSS OFF	PSS ON	PSS OFF	PSS ON	PSS OFF	PSS ON	PSS OFF	PSS ON	PSS OFF	PSS ON	PSS OFF	PSS ON	PSS OFF
Equal sharing	No Fault	1.00	1.00	1.00	1.00	1.00	1.00	1.00	1.00	1.00	1.00	1.00	1.00	1.00	1.00
60% - 40%		1.00	1.00	1.00	1.00	1.00	1.00	1.00	1.00	1.00	1.00	1.00	1.00	1.00	1.00
Equal sharing	Plant 1	0.59	0.16	0.62	0.15	0.64	0.10	0.67	0.11	0.66	0.16	0.61	0.07	0.42	0.07
60% - 40%		0.67	0.09	0.56	0.09	0.70	0.14	0.64	0.14	0.63	0.08	0.73	0.08	0.46	0.10
Equal sharing	Plant 2	0.27	0.00	0.22	0.00	0.33	0.04	0.36	0.05	0.27	0.00	0.26	0.04	0.12	0.07
60% - 40%		0.65	0.09	0.62	0.07	0.66	0.11	0.63	0.13	0.63	0.08	0.73	0.08	0.50	0.07
Equal sharing	Plant 3	0.72	0.79	0.88	0.63	0.78	0.66	0.66	0.66	0.88	0.79	0.56	0.45	0.50	0.42
60% - 40%		0.82	0.75	0.81	0.74	0.77	0.50	0.70	0.65	0.78	0.79	0.73	0.60	0.67	0.52
Equal sharing	Plant 4	0.74	0.72	0.85	0.55	0.74	0.58	0.64	0.37	0.85	0.69	0.72	0.42	0.50	0.52
60% - 40%		0.80	0.71	0.87	0.75	0.77	0.61	0.62	0.62	0.88	0.77	0.70	0.55	0.63	0.53
Equal sharing	Bus 8	0.88	0.66	0.92	0.69	0.90	0.82	0.81	0.65	0.92	0.78	0.87	0.67	0.73	0.54
60% - 40%		0.81	0.82	0.82	0.84	0.90	0.67	0.84	0.75	0.82	0.78	0.87	0.79	0.71	0.66